Egyptian Journal of Chemistry
http://ejchem.journals.ekb.eg/

Melodorum fruticosum Lour. Leaves Methanolic Extract Ameliorates Gentamicin-Induced Renal Toxicity in Rats via Antioxidant, Anti-Inflammatory, and Anti-Apoptotic Pathways

Shaza A. Mohamed [1*], Fatma Abo-Elghiet [1], Samah Fathy Ahmed [2], Ekram Nemr Abd Al Haleem [3], Walid Hamdy El-Tantawy [2] and Noha A. E. Yasin [4]

[1]Pharmacognosy and Medicinal Plants Department, Faculty of Pharmacy (Girls), Al-Azhar University, Cairo, Egypt
[2]National Organization for Drug Control and Research, Cairo, Egypt
[3]Pharmacology and Toxicology Department, Faculty of Pharmacy (Girls), Al-Azhar University, Cairo, Egypt
[4]Cytology and Histology Department, Faculty of Veterinary Medicine, Cairo University, Giza, Egypt

Abstract

Gentamicin, a common remedy for Gram-negative bacterial infections, is clinically hindered by its kidney-related drawbacks. *Melodorum fruticosum* Lour. (*M. fruticosum*), is a plant of Annonaceae family, extensively dispersed in Southeast Asia. This study investigated the renal protective effects of *M. fruticosum* leaves methanolic extract against gentamicin-induced kidney damage in rats. The experiment involved 40 rats divided into control, gentamicin-treated, extract-treated (200 mg/kg and 400 mg/kg) in addition to gentamicin, and reference drug (N-acetyl cysteine, 150 mg/kg) in addition to gentamicin groups. The extract and reference drug were administered for 15 days, while gentamicin was intraperitoneally injected at 100 mg/kg over six days. Gentamicin administration elevated kidney function markers, oxidative stress, inflammation, and cell death indicators. Antioxidant enzyme activities decreased, alongside histopathological changes. Both extract doses and the reference drug mitigated these effects, with the higher extract dose (400 mg/kg) showing better results. The extract's phenolic content (74.35 ± 3.43 mg gallic acid equivalent/g) was quantified following Folin-Ciocalteu procedure while flavonoid content (39.03 ± 2.15 mg catechin equivalent/g) was determined using aluminium chloride colorimetric method. Utilizing advanced, highly sensitive ultraperformance liquid chromatography/electrospray ionization-quadrupole time-of-flight tandem mass spectrometry (UPLC/ESI-QTOF-MS/MS) analysis, 39 phenolic compounds were identified in *M. fruticosum* extract, primarily including flavonoids and phenolic acids.
These findings position *M. fruticosum* extract as a potential therapeutic option for managing kidney disorders and toxicities.

Keywords: *Melodorum fruticosum* Lour.extract, Nephroprotective, Oxidative stress, Inflammation.

1. **Introduction**

Gentamicin (GM) is a widely used aminoglycoside antibiotic that has been proven to be effective against Gram-negative bacteria for over 50 years. It is recommended as the first-line antibiotic for different serious and life-threatening disorders. Although it is clinically effective with low resistance rates, and being affordable, its use is limited by the risk of adverse effects, such as ototoxicity and nephrotoxicity [1, 2]. Many reports suggest that GM treatment for more than seven days can cause acute tubular injury and kidney dysfunction and induce nephrotoxicity in 10–20 % of treated patients, thereby restricting its prolonged clinical application

*Corresponding author e-mail: Shazahalim2652.el@azhar.edu.eg (Shaza A. Mohamed)
Received date 04 May 2024; revised date 29 May 2024; accepted date 04 June 2024
DOI: 10.21608/EJCHEM.2024.287196.9674

[3]. Drug-induced nephrotoxicity remains a major problem, as nephrotoxic drugs are unavoidable in clinical settings. Although antibiotics are crucial for both preventing and treating many diseases and infections, they can also have some unfavorable side effects. GM can break the respiratory chain, cause the overproduction of free radicals, promote cellular necrosis, and activate the apoptotic pathway [4]. It accumulates in the proximal convoluted tubules (PCT) [5] and may result in renal damage [6]. GM also increases leukocyte infiltration, cytokine release, and activating pro-inflammatory factors [7] that may lead to remote organ injury, such as liver injury with a substantial increase in the levels of hepatic enzymes [8].

In recent decades, herbal medicines have increased exponentially and gained popularity in both developed and developing countries. Medicinal plants have curative properties with minimal side effects due to the presence of various complex chemical substances [9]. *M. fruticosum* is a plant species in the Annonaceae family, commonly known as White Cheesewood, and widely distributed in Southeast Asia, particularly in Vietnam, Cambodia, Laos, and Thailand. The essential oil composition of *M. fruticosum* flowers was investigated by GC–MS with eighty-eight identified volatile constituents. Phenyl butanone, linalool, benzyl alcohol, α-cadinol, globulol and viridiflorol were found to be the major components, respectively [10]. *M. fruticosum* is a versatile plant with several uses. Its edible fruits can be utilized to make drinks and wines, while its fragrant flowers are used in perfumes. Vietnamese traditional medicine has long employed the plant's dried flowers as a blood tonic and its leaves as a digestive aid [11]. Previous phytochemical studies on this plant have led to the isolation of terpenoids, aromatic compounds, butenolides, heptenoids, aporphine alkaloids, and flavonoids. Three new flavonoid derivatives, Melodorones A–C, together with four known compounds, tectochrysin, chrysin, onysilin, and pinocembrin were isolated from the stem bark of *M. fruticosum*. The plant exhibits antifungal, anti-inflammatory, and antioxidant properties [12].

To date, the potential protective effect of *M. fruticosum* against GM-induced nephrotoxicity has not been explored. Therefore, the current study aimed to determine whether *M. fruticosum* leaves methanolic extract has an ameliorative effect against GM-induced nephrotoxicity in rats and to explore the possible underlying mechanism of its action. This study also characterized the chemical profile of the mentioned extract using UPLC/ESI-QTOF-MS/MS analysis, determined its total phenolic and flavonoid contents, and studied its *in vitro* and *in vivo* antioxidant activity.

2. Materials and Methods

2.1. Chemicals

GM sulphate is commercially available as Epigent (80 mg/2 ml ampoules) from the Egyptian International Pharmaceutical Industries Co. (EIPICo.), 10th of Ramadan City, Egypt. 2,2-Diphenyl-1-picrylyhydrazyl (DPPH), N-acetyl cysteine, Folin-Ciocalteu reagent, gallic acid, and catechin were obtained from Sigma Aldrich (St. Louis, MO). All chemicals used in the current study were of the highest analytical grade.

2.2. Plant material

The leaves of *Melodorum fruticosum* Lour. (Annonaceae) were obtained from a private botanical garden in Cairo, Egypt in April 2020 with due permission obtained from the garden as per institutional, national, and international guidelines. The plant's identification was confirmed by Dr. Trease Labeb, senior specialist of plant taxonomy, El-Orman Botanical Garden, Giza, Egypt. A voucher specimen (Mf-2020) was deposited at the herbarium of the Department of Pharmacognosy and Medicinal Plants, Faculty of Pharmacy (Girls), Al-Azhar University, Cairo, Egypt.

2.3. Preparation of *M. fruticosum* methanolic extract

The air-dried and pulverized leaves of *M. fruticosum* (0.5 kg) were soaked and extracted with methanol (2 L x 3 times). The resulting extract was filtered and evaporated to dryness under a vacuum at 50°C.

2.4. Phytochemical screening

Standard chemical tests were used to screen the leaves of *M. fruticosum* for the presence or absence of various phytoconstituents, such as carbohydrates, glycosides, saponins, tannins, flavonoids, sterols, triterpenes, anthraquinones, and alkaloids [13].

2.5. *In vitro* antioxidant activity (DPPH$^{\bullet}$ scavenging assay)

To evaluate the radical scavenging activity of the *M. fruticosum* leaves methanolic extract, the stable DPPH radical was used, with rutin as the reference standard [14]. The antioxidant activity of the extract was expressed as the percentage inhibition of the DPPH radical, and the IC_{50} value was calculated using probit analysis [15].

2.6. Estimation of total phenolic and flavonoid contents

To determine the total phenolic content of the *M. fruticosum* leaves methanolic extract, the Folin-Ciocalteu procedure was employed [16]. Gallic acid was used as the standard for the calibration curve, and the results were expressed as mg of gallic acid equivalent per gram of extract (mg GAE/g). Meanwhile, the total flavonoid content was determined using the aluminium chloride colorimetric method [17]. Catechin was used to perform the calibration curve, and the results were expressed as mg of catechin equivalent per gram of extract (mg CE/g).

2.7. UPLC/ESI-QTOF-MS/MS analysis

To identify secondary metabolites in the *M. fruticosum* leaves methanolic extract, ultraperformance liquid chromatography-electrospray ionization-quadrupole time-of-flight tandem mass spectrometry (UPLC/ESI-QTOF-MS/MS) was used in negative ionization mode. The various phytoconstituents in the extract were tentatively identified by comparing their tandem mass spectral data to databases, ReSpect negative (which contains 1573 records), as well as by comparing their fragmentation patterns to those of previously reported phytoconstituents [18].

2.8. Animals

Male albino Wistar rats, aged 12 weeks and weighing approximately 165-185 g, were housed in plastic cages with a relative humidity of 50-55%, temperature of 25℃, and a 12-hour light-12-hour dark cycle. They were provided with *ad libitum* access to a standard rodent pellet and drinking water. All *in vivo* treatments and experiments were approved by the Institutional Animal Care and Use Committee of the Veterinary Medicine at Cairo University (Vet Cu 2009 2022485) and adhered to National Institutes of Health regulations. All methods were performed in accordance with Animal Research: Reporting of *In Vivo* Experiments (ARRIVE) guidelines.

2.9. Acute toxicity study

An acute toxicity study was conducted [19] to assess the potential toxicity of the methanolic extract of *M. fruticosum* leaves and determine a safe dosage range for consequent experiments. In a preliminary experiment, three groups of 10 rats each received doses of 5, 50, and 500 mg/kg of the tested extract suspended in a 2% v/v Tween 80 vehicle. Animals were monitored for 24 h for signs of toxicity (diarrhoea, nausea, vomiting, queasiness, restlessness, fever, sleepiness, confusion, collapsing, and convulsions) and mortality. Based on the findings of the preliminary experiment, other groups of 10 rats each were subjected to higher doses of the examined extract (600, 1000, 2000, and 4000 mg/kg). Control animals received only the vehicle and were remained under identical conditions. Signs of toxicity and mortality rates were recorded within 24 hours for each dose.

2.10. Experimental design

In this study, forty male albino Wistar rats were randomly distributed into five groups of eight rats each. The groups were categorized as follows:

- **I.** Control group (C): Rats received only an oral treatment of distilled water.
- **II.** GM-treated group (GM): Rats were administered intraperitoneal (i.p.) injections of GM (100 mg/Kg body weight) for six consecutive days [8].
- **III.** Low dose extract in addition to GM group (LDE + GM): Rats were orally administered 200 mg/Kg body weight of *M. fruticosum* leaves methanolic extract once a day for 15 days using a gastric tube. GM was given at a dose of 100 mg/kg from the third day for six consecutive days [20].
- **IV.** High dose extract in addition to GM group (HDE + GM): Rats were orally administered 400 mg/Kg body weight of *M. fruticosum* leaves methanolic extract once a day for 15 days using a gastric tube. GM was given at a dose of 100 mg/kg from the third day for six consecutive days [20].
- **V.** N-acetyl cysteine in addition to GM group (NAC + GM): Rats were orally administered 150 mg/Kg body weight of N-acetyl cysteine (NAC) as a reference

drug once a day for 15 days using a gastric tube [21]. GM was given at a dose of 100 mg/kg from the third day for six consecutive days.

2.11. Blood collection and biochemical assays

On day 16 of the experimental period, blood samples were collected from the retro-orbital veins of each animal and allowed to clot for 1 hour before being centrifuged for 20 minutes at 3,000 rpm. Rats were anesthetized by i.p. injection of pentobarbitone sodium (60 mg/kg) and sacrificed by cervical dislocation. Kidneys were dissected immediately and weighed using an electronic balance. Subsequently, kidney tissue samples were used for further biochemical and histopathological examination. Commercial kits purchased from Diamond, Cairo, Egypt, were used to determine the levels of urea, blood urea nitrogen (BUN), creatinine, alanine aminotransferase (ALT), and aspartate aminotransferase (AST) in the obtained serum samples.

2.12. Biochemical analysis

The kidney tissue samples were homogenized in ice-saline to prepare a concentration of 10% (w/v). The obtained homogenates were then centrifuged for 20 minutes at 4°C and 6,000 ×g. The renal protein content was assessed using Lowry's method [22], with bovine serum albumin as a standard.

The tissue homogenate was utilized to measure the level of reduced glutathione (GSH) [23], malondialdehyde (MDA) [24], superoxide dismutase activity (SOD) [25], catalase (CAT) activity [26], glutathione-S-transferase (GST) activity [27], nitric oxide levels (NO) [28] and myeloperoxidase (MPO) activity [29, 30]. ELISA kits purchased from Cusabio, Germany were used to determine NF-κB, TNF-α, IL-6, and caspase-3 levels.

2.13. Histopathological studies

The collected kidney specimens were preserved in 10% neutral buffered formalin for a period of 24 - 48 hours. Then, they were processed using different grades of alcohol (70-100%) and xylene, embedded in paraffin wax, and sliced into 4 µm sections. Subsequently, these sections were stained with hematoxylin and eosin (H&E) [31]. Finally, the stained sections were examined, and the photomicrographs were captured using a camera (LEICA ICC50 HD) attached to a light microscope (LEICA DM500) at Cytology & Histology Department Faculty of Veterinary Medicine Cairo University.

A conventional semi-quantitative scoring system was used to score the notable histological changes and the severity of lesions among different experimental groups (n=8 rats/group). The scoring system was as follows: (0) represents no histological changes (normal), whereas (1), (2), (3), and (4) denoted varying degrees of mild tissue damage (< 25%), moderate tissue damage (25% - 50%), severe tissue damage (50% - 75%), and extremely severe tissue damage (> 75%) [32]. The criteria utilized to assess renal damage were renal tubular degeneration and necrosis, inflammatory cell infiltration, and hyaline casts.

2.14. Immunohistochemical detection of caspase 3 and NF-κB

Kidney paraffin-embedded sections were affixed onto adhesive slides and subjected to immunohistochemistry staining (IHC). The sections were rehydrated and subjected to antigen retrieval by heating for 15 minutes. Primary antibodies, including Anti caspase 3/CPP32, active form (Diagnostic BioSystems), and Anti NFκB-p65 (Elabscience Biotechnology), were incubated at a dilution of 1:100 overnight. The sections were then washed and incubated with horse radish peroxidase (Goat Anti-Rat IgG, abcam company) (secondary antibody) for 2 hours. The immunostaining was developed using a diaminobenzidine kit, and positive immunoreactivity was indicated by a brown colour.

For image analysis, seven IHC-stained kidney sections (×400) from each group were examined. The ImageJ program was used to quantify the area percentage (area %) of positive immunoreactivity.

2.15. Statistical analysis

The statistical analysis was conducted using SPSS version 21.0, involving a one-way analysis of variance (ANOVA) followed by Tukey's multiple comparison test. The results were expressed as mean ± standard error of the mean (SEM). The non-parametric data of histopathological lesion scores were presented as the median ± the interquartile range. The Kruskal-Wallis test and the Mann-Whitney U test were used to statistically analyse the data [33]. Statistical significance was determined for *P* values less than 0.05. The correlation coefficient was calculated using linear regression [34].

3. Results

3.1. Phytochemical screening

Carbohydrates and/or glycosides, tannins, flavonoids, saponins, triterpenes, and alkaloids were detected in the preliminary phytochemical screening of *M. fruticosum* leaves.

3.2. *In vitro* antioxidant activity

The *in vitro* antioxidant activity of the *M. fruticosum* leaves methanolic extract was assessed using the DPPH˙ scavenging assay with rutin as a reference standard. Results showed that the extract's free radical scavenging ability was concentration-dependent, with an IC_{50} value of 75.79 µg/ml. In comparison, the reference standard rutin had an IC_{50} value of 3.79 µg/ml **(Fig.1).**

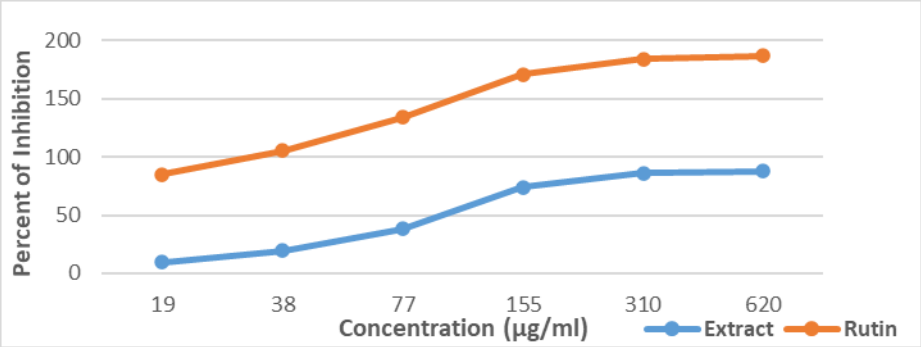

Fig. 1. DPPH˙ scavenging activity of *M. fruticosum* leaves methanolic extract

3.3. Total phenolic and total flavonoid contents

The total phenolic and flavonoid contents of the *M. fruticosum* leaves methanolic extract were determined and presented in **(Table 1)**. The phenolic content was measured to be 74.35 ± 3.43 mg GAE/g, while the total flavonoid content was found to be 39.03 ± 2.15 mg CE/g after using the gallic acid (R^2 = 0.9976), and catechin (R^2 = 0.9994) calibration curves, respectively.

Table 1. Total phenolic and total flavonoid contents of *M. fruticosum* leaves methanolic extract:

Total phenolic content	74.35 ± 3.43 mg GAE/g
Total flavonoid content	39.03 ± 2.15 mg CE/g

Values are expressed as mean ± SEM of three replicates. GAE: Gallic acid equivalent, CE: Catechin equivalent.

3.4. UPLC-ESI-QTOF-MS/MS analysis

The chemical profile of the *M. fruticosum* methanolic extract was analysed using the negative ionization mode of the UPLC/ESI-QTOF-MS/MS technique. A total of 39 compounds were tentatively identified, with the majority being phenolic compounds. Of the identified compounds, 36 were phenolics, while the remaining three were organic acids and sugar alcohol. The phenolic compounds were categorized into flavonoids, coumarin, furanochromones, phenolic acids, and phenolic amides. Compounds were identified by comparing their molecular weight and fragmentation pattern with those of previously reported constituents through tandem mass spectral databases and published data. The chromatogram of the *M. fruticosum* methanolic extract, and a comprehensive list of the identified compounds arranged in order of their retention time were illustrated **(Fig. 2 and Table 2)** respectively.

Flavonoids were the chief constituents of the *M. fruticosum* leaves methanolic extract, with flavonols, flavones, flavanones, and chalcones being the most prominent subclasses. Among the identified flavonols, kaempferol was detected at R_t = 10.81 min with a parent ion $[M-H]^-$ at *m/z* 285.0417, which corresponds to the molecular formula $C_{15}H_{10}O_6$. Its MS^2 fragmentation generated two daughter ions at *m/z* 255 for $[M-H-30]^-$ and at *m/z* 227 for CO elimination from the fragment ion at *m/z* 255 **(Fig. 3a)** [35]. Quercetin, on the other hand, was eluted at R_t = 9.55 min with $[M-H]^-$ at *m/z* 301.0359, matching the molecular formula $C_{15}H_{10}O_7$. Its MS^2 fragmentation yielded two daughter ions at *m/z* 179 for $[^{1,2}A]^-$ and at *m/z* 151 for $[^{1,3}A]^-$ **(Fig. 3b)** [36]. Furthermore, Rutin, a glucosyl–rhamnosyl quercetin, was detected at R_t = 6.05 min with $[M-H]^-$ at *m/z* 609.1447, representing the molecular formula $C_{27}H_{30}O_{16}$. It also showed a characteristic fragment ion at *m/z* 300 representing the radical quercetin anion resulting from the loss of both glucosyl and rhamnosyl moieties **(Fig. 3c)** [36].

Of the identified flavones, luteolin (R_t = 9.32 min) exhibited a molecular ion peak $[M-H]^-$ at *m/z* 285.0408 consistent with the molecular formula $C_{15}H_{10}O_6$ and a fragment ion peak at *m/z* 133 for $[^{1,3}B]^-$ **(Fig. 3d)** [37]. Furthermore, apigenin (R_t = 10.53 min) showed $[M-H]^-$ at *m/z* 269.0456 for the molecular formula $C_{15}H_{10}O_5$, along with daughter ions at *m/z* 149 for $[^{1,4}B^-+2H]$ and at *m/z* 117 for $[^{1,3}B]^-$ **(Fig. 3e)** [37]. Another prevalent flavone in *M. fruticosum* is chrysin, which was detected at R_t 13.12 min with molecular ion peak $[M-H]^-$ at *m/z* 253.0506 representing the molecular formula $C_{15}H_{10}O_4$. It further suffered a neutral loss of 44 Da (CO_2) yielding the fragment ion at *m/z* 209 for $[M-H-CO_2]^-$. The fragment ion at *m/z* 181 resulted from the consecutive loss of CO from the ion at *m/z* 209 **(Fig. 3f)** [12, 37].

Among the flavanones detected in *M. fruticosum*, naringenin and pinocembrin were present. Naringenin was eluted at 10.25 min and exhibited a precursor ion $[M-H]^-$ at *m/z* 271.0619 matching the molecular formula $C_{15}H_{12}O_5$. It also generated a fragment ion [M-H-ring B] $^-$ at *m/z* 177 corresponding to the loss of B ring. The ions at *m/z* 151 and *m/z* 119 are typically due to the retro-Diels–Alder (RDA) cleavage between the chemical bonds 1 and 3 of the C ring **(Fig. 3g)** [37]. Pinocembrin is another abundant flavanone detected in *M. fruticosum*, which was previously isolated from it [38], had a retention time of 13.00 min and displayed a parent ion $[M-H]^-$ at *m/z* 255.0661, indicating the molecular formula $C_{15}H_{12}O_4$. Upon further MS-MS fragmentation, the parent ion produced fragment ions $[M-H-C_2H_2O]^-$ at *m/z* 213, resulting from the loss of 42 Da (C_2H_2O group), and a fragment ion at *m/z* 151 for $[^{0,2}A]^-$ **(Fig. 3h)** [39].

Ferulic acid, which is among the most abundant phenolic acids found in the *M. fruticosum* leaves methanolic extract, exhibited a precursor ion $[M-H]^-$ at *m/z* 193.0496, confirming its molecular formula as $C_{10}H_{10}O_4$. Upon MS^2 fragmentation, characteristic product ions such as $[M-H-CH_3]^-$ at *m/z* 178, $[M-H-CH_2-H_2O]^-$ at *m/z* 161, and $[M-H-CH_3-CO_2]^-$ at *m/z* 134 **(Fig. 3i)** [40]. Additionally, melodamide A, a phenolic amide previously isolated from *M. fruticosum*, was detected at 10.61 min with a molecular ion $[M-H]^-$ at *m/z* 282.1132 consistent with the molecular formula $C_{17}H_{17}NO_3$ [41]. Its tandem mass spectrum showed production at *m/z* 178 for $[C_9H_8NO_3]^-$, which subsequentially lost the amide group to yield a fragment ion at *m/z* 135 **(Fig. 3j).**

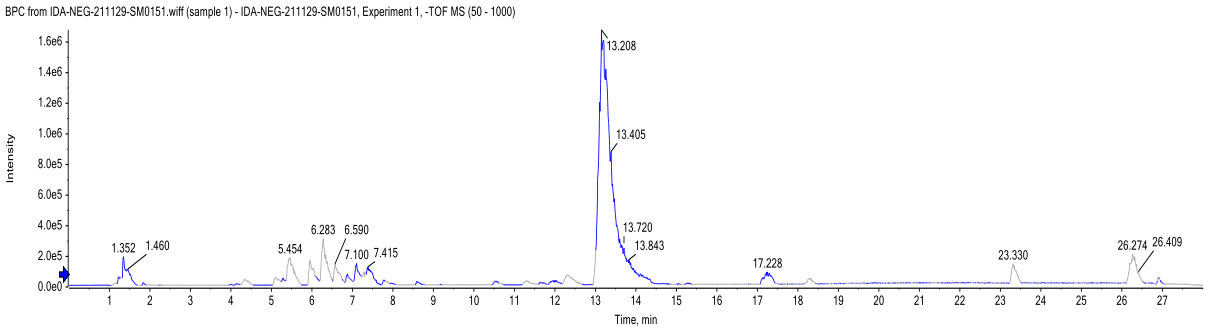

Fig 2. Base peak chromatogram (BPC) of *M. fruticosum* leaves methanolic extract using UPLC/ESI-QTOF-MS/MS technique in negative ionization mode

Table 2. Tentatively identified secondary metabolites from *M. fruticosum* leaves:

No.	Tentatively identified compounds	R_t (min)	Precursor *m/z* $[M-H]^-$	Elemental composition	Fragmentation	Chemical Class
1	Malic acid	0.98	133.0140	$C_4H_6O_5$	115, 73, 71	Organic acid
2	Quinic acid	1.11	191.0561	$C_7H_{12}O_6$	173, 127, 85	Organic acid
3	Protocatechuic acid	1.19	153.0181	$C_7H_6O_4$	112, 109, 108	Phenolic acid
4	Mannitol	1.24	181.0713	$C_6H_{14}O_6$	163, 119, 101, 71, 59	Sugar alcohol
5	Chlorogenic acid	1.35	353.0879	$C_{16}H_{18}O_9$	191, 179, 173	Phenolic acid
6	4-Hydroxycinnamic acid	1.36	163.0387	$C_9H_8O_3$	119	Phenolic acid
7	Benzoic acid	1.51	121.0285	$C_7H_6O_2$	93, 77	Phenolic acid
8	P-hydroxy benzoic acid	2.91	137.0235	$C_7H_6O_3$	93	Phenolic acid
9	Esculin	3.78	339.0723	$C_{15}H_{16}O_9$	177, 133	Coumarin
10	Aesculetin	5.03	177.0190	$C_9H_6O_4$	133	Coumarin
11	Flavokawin A	5.13	315.1078	$C_{18}H_{20}O_5$	269, 161, 71	Chalcone
12	Epicatechin	5.45	289.0715	$C_{15}H_{14}O_6$	245, 221, 203, 179, 153, 123, 113	Flavanol
13	Rutin	6.05	609.1447	$C_{27}H_{30}O_{16}$	300	Flavonol
14	Quercetin-3-*O*-pentosylhexoside	6.12	595.1292	$C_{26}H_{28}O_{16}$	300, 271, 179	Flavonol
15	Norvisnagin	6.45	215.0348	$C_{12}H_8O_4$	187	Furanochromones
16	Kaempferol-7-neohesperidoside	6.47	593.1511	$C_{27}H_{30}O_{15}$	285, 255	Flavonol
17	Spiraeoside (quercetin-4'-hexoside)	6.64	463.0888	$C_{21}H_{20}O_{12}$	301, 300, 271	Flavonol
18	Guaijaverin (quercetin-3-D-pentoside)	7.12	433.0784	$C_{20}H_{18}O_{11}$	301, 300, 271, 255, 179	Flavonol
19	Astragalin (kaempferol-3-hexoside)	7.22	447.0927	$C_{21}H_{20}O_{11}$	285, 284, 255, 227	Flavonol
20	Quercitrin	7.27	447.0922	$C_{21}H_{20}O_{11}$	301, 300, 271	Flavonol
21	Phlorizin	7.87	435.1280	$C_{21}H_{24}O_{10}$	273, 167	Chalcone
22	Afzelin	8.06	431.0984	$C_{21}H_{20}O_{10}$	285, 255, 227	Flavonol
23	2',4'-Dihydroxy-4,6'-dimethoxydihydrochalcone	8.16	301.1201	$C_{17}H_{18}O_5$	255, 195, 167	Chalcone
24	Ferulic acid	8.65	193.0496	$C_{10}H_{10}O_4$	178, 161, 134, 133	Phenolic acid
25	*p*-coumaroyltyramine	8.93	282.1137	$C_{17}H_{17}NO_3$	162, 136, 119	Phenolic amide
26	Luteolin	9.32	285.0408	$C_{15}H_{10}O_6$	133	Flavone
27	Quercetin	9.55	301.0359	$C_{15}H_{10}O_7$	179, 151, 121	Flavonol
28	Naringenin	10.25	271.0619	$C_{15}H_{12}O_5$	177, 151, 119	Flavanone
29	Tectochrysin	10.3	267.0659	$C_{16}H_{12}O_4$	252	Flavone
30	Phloretin	10.37	273.0670	$C_{15}H_{14}O_5$	167	Chalcone
31	Hesperetin	10.38	301.0697	$C_{16}H_{14}O_6$	286, 257, 164, 151	Flavanone
32	Apigenin	10.53	269.0456	$C_{15}H_{10}O_5$	149, 117	Flavone
33	Melodamide A	10.61	282.1132	$C_{17}H_{17}NO_3$	178, 135	Phenolic amide
34	Kaempferol	10.81	285.0417	$C_{15}H_{10}O_6$	255, 227	Flavonol
35	Diosmetin (luteolin 4'-methyl ether)	12.48	299.0564	$C_{16}H_{12}O_6$	284, 256	Flavone
36	Pinocembrin	13.00	255.0661	$C_{15}H_{12}O_4$	213, 211, 187, 171, 151, 145	Flavanone
37	Baicalein	13.08	269.0438	$C_{15}H_{10}O_5$	241, 225, 197, 183, 169	Flavone
38	Chrysin	13.12	253.0506	$C_{15}H_{10}O_4$	209, 181, 145, 143	Flavone
39	7,4′-dihydroxy-5-methoxyflavanone	13.87	285.0754	$C_{16}H_{14}O_5$	165, 119, 93	Flavanone

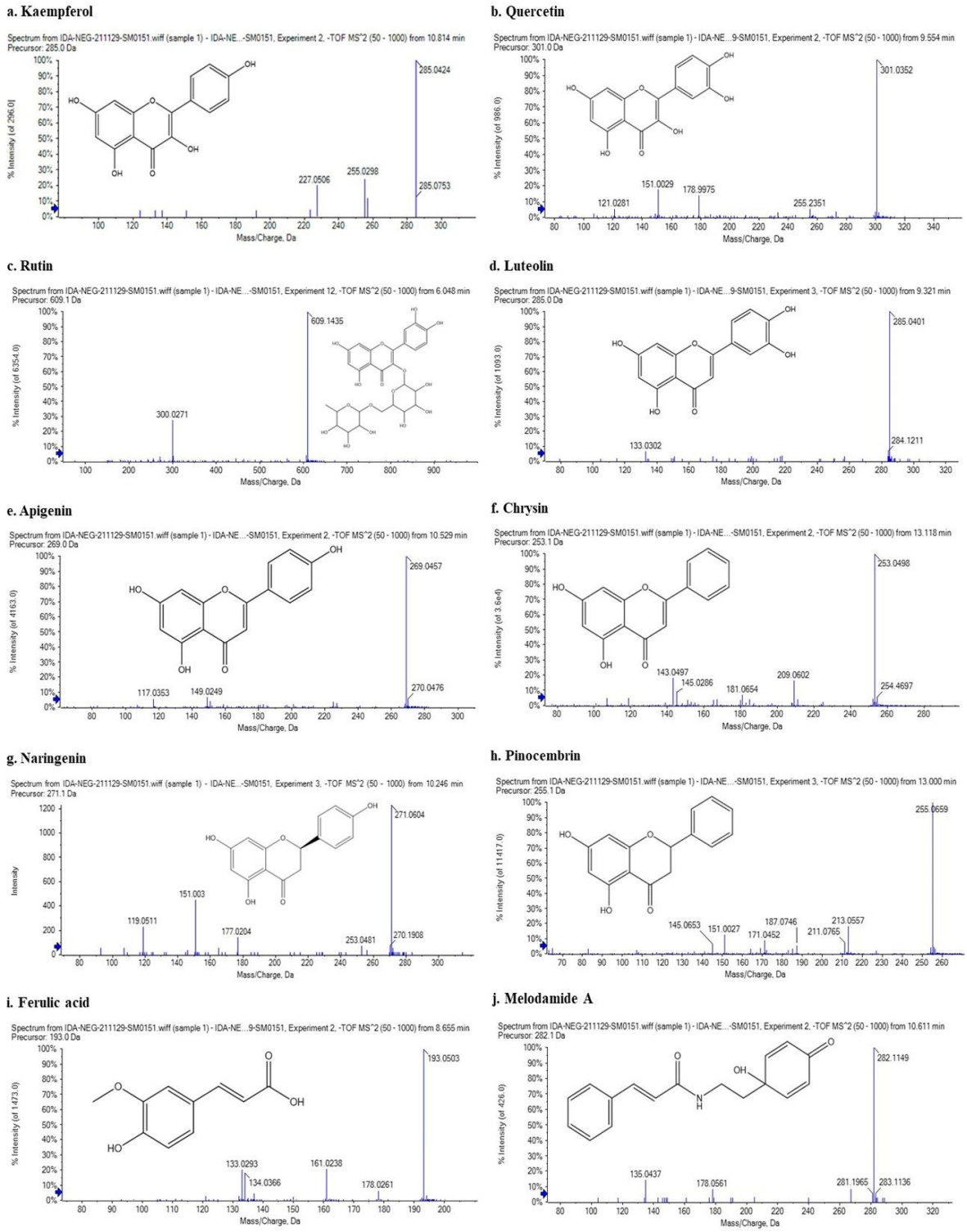

Fig. 3. Mass spectra of the most bioactive components identified in the methanolic leaves extract of *M. fruticosum*

3.5. Acute toxicity study

Throughout the experimental period, neither behavioural changes nor mortality rates were recorded in rats that were administered doses up to 4000 mg/kg body weight of the *M. fruticosum* leaves methanolic extract. Consequently, further studies were conducted using doses of 200 and 400 mg/kg body weight (the recommended therapeutic doses were chosen as 1/20 and 1/10 of the calculated LD_{50}).

3.6. Effect of treatment on the serum levels of urea, BUN, creatinine, BUN/creatinine ratio, ALT, and AST

Intraperitoneal injection of the GM significantly ($P < 0.05$) increased the serum urea, BUN, creatinine, and BUN/creatinine ratio, ALT, and AST compared to their corresponding controls. Whereas the pre-treatment with both doses of the *M. fruticosum* methanolic extract, as well as NAC, caused a significant ($P < 0.05$) decline in their serum levels compared to the GM-treated rats. Interestingly, there were no significant differences in the serum levels of these parameters compared to the control group, except for the ALT and AST levels in the LDE and NAC groups, which showed a significant difference from the control group at ($P < 0.05$), **(Table 3).**

Table 3. Serum urea, BUN, creatinine level, BUN/creatinine ratio, ALT, and AST activities in different experimental groups:

Parameters	C	GM (100 mg/Kg)	LDE+GM (200 mg/Kg + 100 mg/Kg)	HDE+GM (400 mg/Kg + 100 mg/Kg)	NAC+GM (150 mg/Kg + 100 mg/Kg)
Urea (mg/dl)	34.17 ± 0.94	40.05 ± 0.71 [a]	36.03 ± 1.12 [b]	34.92 ± 0.67 [b]	35.61 ± 0.93 [b]
BUN (mg/dl)	15.95 ± 0.48	18.7 ± 0.36 [a]	16.82 ± 0.57 [b]	16.3 ± 0.34 [b]	16.62 ± 0.47 [b]
Creatinine (mg/dl)	0.62 ± 0.02	1.02 ± 0.05 [a]	0.72 ± 0.04 [b]	0.65 ± 0.04 [b]	0.70 ± 0.02 [b]
BUN/Creatinine ratio	25.66 ± 1.14	18.5 ± 0.95 [a]	23.46 ± 0.79 [b]	25.73 ± 1.6 [b]	23.74 ± 1.22 [b]
ALT (U/L)	23.60 ± 0.75	59.64 ± 1.55 [a]	31.19 ± 0.79 [abc]	25.40 ± 0.42 [bd]	30.80 ± 0.8 [ab]
AST (U/L)	34.60 ± 0.59	86.00 ± 1.79 [a]	43.93 ± 0.58 [abc]	36.47 ± 0.84 [b]	40.13 ± 1.39 [ab]

Results are presented as Mean ± S.E.M, (n = 8 rats/group). [a] Significantly different from control, [b] Significantly different from GM-treated group, [c] Significantly different from HDE + GM-treated group, [d] Significantly different from NAC + GM-treated group, the same superscript letters in the same row are considered insignificant. The statistical analysis was conducted using (ANOVA) followed by Tukey's multiple comparison test.

3.7. Effect of treatment on GSH, SOD, GST, and CAT in renal homogenate

The GM intoxication markedly ($P < 0.05$) decreased the GSH, SOD, GST, and CAT activities compared to the control group. Conversely, the administration of the *M. fruticosum* extract and NAC significantly ($P < 0.05$) increased the level of these parameters compared to the GM-treated animals. Concerning the SOD activity, rats receiving the highest dose of the extract showed a significant ($P < 0.05$) increase in its activity compared to those administered with the low dose, **(Table 4).**

3.8. Effect of treatment on renal MDA, NO, MPO, TNF-α, IL-6, caspase-3, and NF-$_k$B

Compared to the control group, the GM-treated group revealed a significant ($P < 0.05$) increase in the renal levels of MDA, NO, myeloperoxidase, TNF-α, IL-6, caspase-3, and NF_kB. However, pre-administration with both doses of the extract and NAC exhibited a marked ($P < 0.05$) decline in their levels compared to the GM-treated rats. Furthermore, rats receiving the highest dose of the extract (400 mg/kg) showed a significant decrease in the MDA, NO, MPO, TNF-α, IL-6, caspase-3, and NF_kB than those receiving the lowest dose (200 mg/kg) **(Table 4 & Fig. 4).**

Table 4. Renal GSH level, SOD, GST, catalase activities, MDA, and NO levels in different studied groups:

Parameters	C	GM (100 mg/Kg)	LDE+GM (200 mg/Kg + 100 mg/Kg)	HDE+GM (400 mg/Kg + 100 mg/Kg)	NAC+GM (150 mg/Kg + 100 mg/Kg)
GSH (nmol/mg protein)	31.05 ± 0.67	26.62 ± 0.18[a]	28.91 ± 0.29 [ab]	30.39 ± 0.39 [b]	30.49 ± 0.37[b]
SOD (U/mg protein)	42.69 ± 1.29	31.96 ± 0.56 [a]	39.46 ± 0.42 [abcd]	44.18 ± 0.55 [b]	43.92 ± 0.71 [b]
GST (nmol/ mg protein)	71.35 ± 0.95	58.97 ± 1.4 [a]	65.5 ± 1.98 [bd]	69.33 ± 1.79 [b]	72.03 ± 0.8 [b]
CAT (U/mg protein)	19.85 ± 0.2	17.81 ± 0.16 [a]	19.49 ± 0.28 [b]	19.83 ± 0.14 [b]	19.99 ± 0.18 [b]
MDA (nmol/g tissue)	82.3 ± 1.65	124.73 ± 1.56 [a]	102.38 ± 1.92 [abcd]	83.19 ± 2.5 [b]	82.48 ± 2.32 [b]
NO (µM/g tissue)	156.27 ± 2.09	179.72 ± 1.6 [a]	167.86 ± 2.06 [abc]	159.42 ± 2.49 [b]	162.64 ± 1.44 [b]

Results are expressed as Mean ± S.E.M, (n = 8 rats/group). [a] Significantly different from control, [b] Significantly different from GM-treated group, [c] Significantly different from HDE + GM-treated group, [d] Significantly different from NAC + GM-treated group, the same superscript letters in the same row are considered insignificant. The statistical analysis was conducted using (ANOVA) followed by Tukey's multiple comparison test.

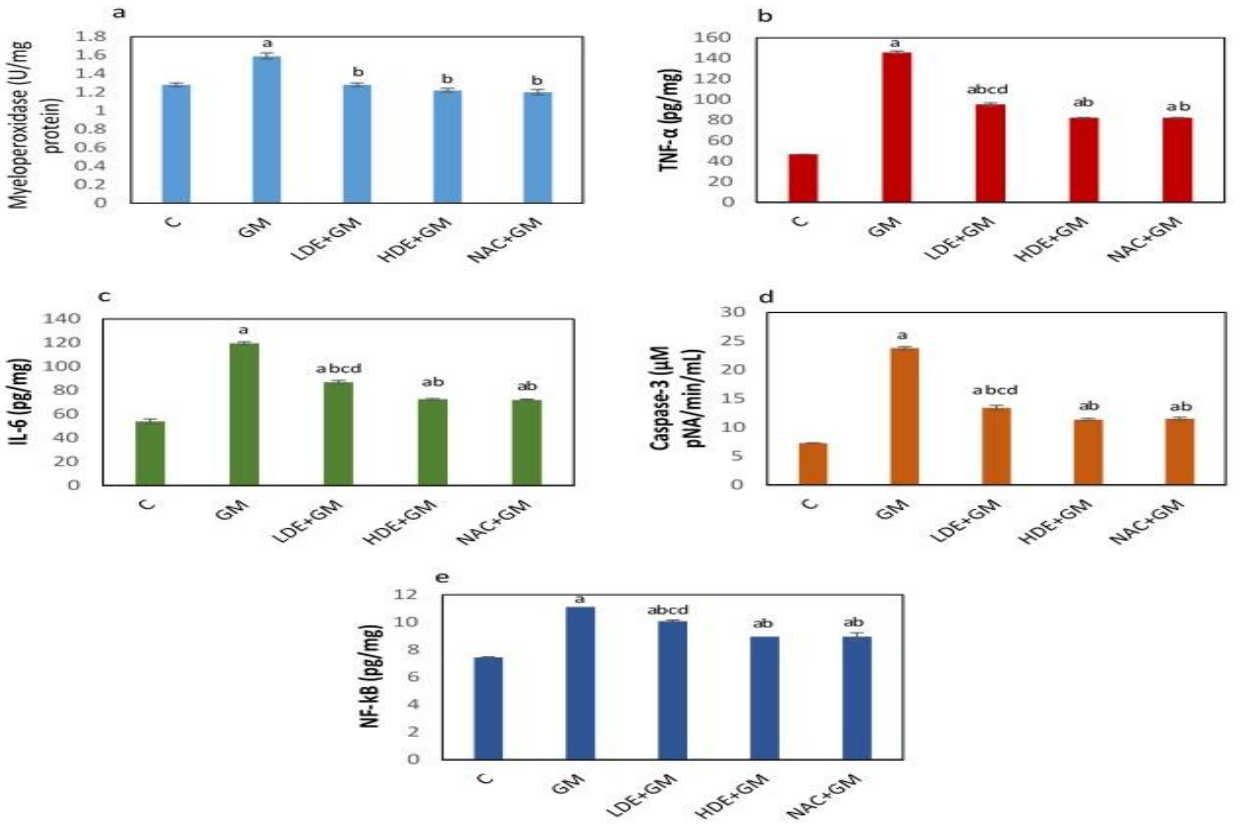

Fig. 4. Myeloperoxidase activity (a), TNF-α level (b), IL-6 level(c), caspase-3 activity (d), and NF-$_k$B level (e) of renal homogenate in different experimental groups:

Results are expressed as Mean ± S.E.M, (n = 8 rats/group). [a] Significantly different from control, [b] Significantly different from GM-treated group, [c] Significantly different from HDE + GM-treated group, [d] Significantly different from NAC + GM-treated group.

3.9. Correlation studies

The Renal MDA level was found to be strongly correlated with the renal GSH level, SOD activity, GST activity, and catalase activity (r = -0.79**, -0.894**, -0.771** and -0.814**, respectively (**P < 0.01). Renal NO level significantly correlated with the renal GSH, SOD, GST, and CAT activities (r = -0.68**, -0.775**, -0.617**, and -0.639**, respectively (**P < 0.01).

3.10. Histopathological investigations

The H&E-stained kidney tissue sections from the control rats displayed normal histological architecture of the renal corpuscle and proximal and distal convoluted tubules **(Fig. 5a).** However, the GM-treated group exhibited severe renal damage, including glomerular degeneration and atrophy with dilated Bowman's space, tubular necrosis, widening of the renal tubules with squamous epithelial cells lining, vacuolar degeneration of renal tubules with desquamation of epithelial lining, edema, severe interstitial inflammatory cells infiltration (interstitial nephritis) and hyalinization **(Fig. 5b-e)**. Conversely, rats co-treated with the low dose of *M. fruticosum* extract (LDE; 200 mg/kg) **(Fig. 5f)**, high dose of *M. fruticosum* extract (HDE; 400 mg/kg) **(Fig. 5g)**, and NAC **(Fig. 5h)** demonstrated remarkable improvement in the histological architecture. Only LDE and NAC groups showed mild to moderate tubular degeneration, mild tubular necrosis, and mild interstitial inflammatory cell infiltration **(Fig. 5f & h, respectively).** Furthermore, the LDE group displayed mild glomerular atrophy and degeneration **(Fig. 5f)**, while the HDE group exhibited a normal architecture of the renal cortex **(Fig. 5g)**.

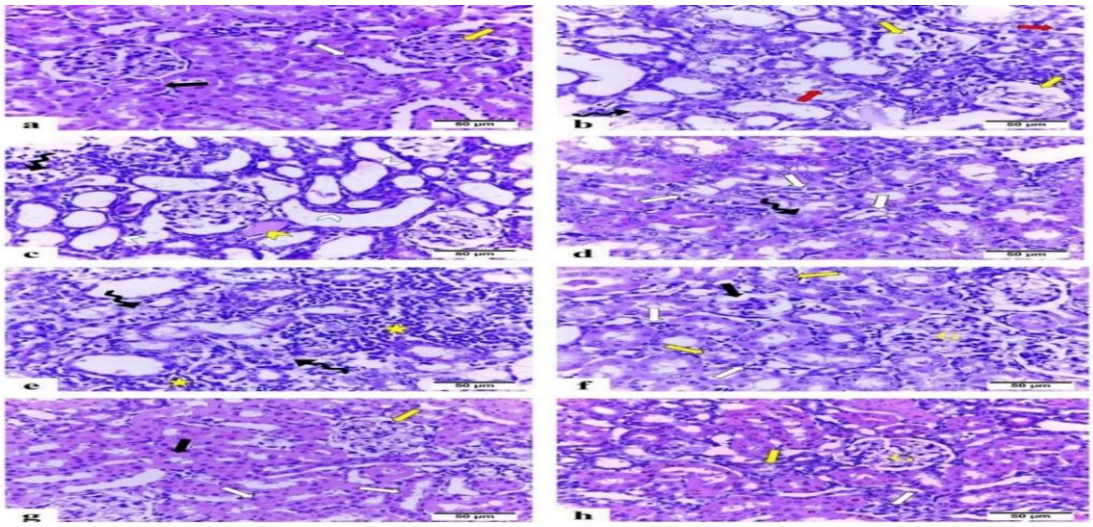

Fig. 5. Representative photomicrographs of renal cortex sections of different experimental groups (H & E):
(a) Control group displays normal histological architecture of renal corpuscle (yellow arrow) and tubules; proximal (black arrow) and distal (white arrow) convoluted tubules. (b-e) GM-treated group exhibits severe renal damage, including glomerular degeneration and atrophy with dilated Bowman's space (yellow arrow), widening of renal tubules with squamous epithelial cells lining (white arrowhead), vacuolar degeneration of renal tubules with desquamation of epithelial lining (red arrow), severe interstitial inflammatory cells infiltration (star), edema (wave arrow) and hyalinization (yellow arrowhead). (f) LDE+ GM-treated group demonstrates remarkable improvement in the histological architecture with mild tubular degeneration (yellow arrow) and mild interstitial inflammatory cells infiltration (white arrow). Moreover, some glomerular corpuscles (G) appear nearly normal while others appear atrophied with dilated urinary space (black arrow). (g) HDE+GM-treated group shows a notable improvement in the histological architecture with apparently normal renal corpuscle (yellow arrow), proximal (black arrow) and distal (white arrow) convoluted tubules. (h) NAC + GM-treated group reveals marked improvement in the cytoarchitecture. Mild tubular degeneration (yellow arrow) and mild inflammatory cells (white arrow) are also observed.

Furthermore, sections of the renal medulla from the control group showed normal architecture of collecting tubules (Fig. 6a). In contrast, the GM-treated group revealed severe vacuolar degeneration of collecting tubules, edema, interstitial inflammatory infiltrates, congestion, and hyaline casts (Fig. 6b). Conversely, the co-treated groups (LDE, HDE, and NAC) displayed the nearly normal architecture of collecting tubules. However, some collected tubules of the LDE group showed mild to moderate vacuolar degeneration (Fig. 6c). Moreover, congestion was observed, but to a lesser extent, in all co-treated groups (Fig. 6c-e).

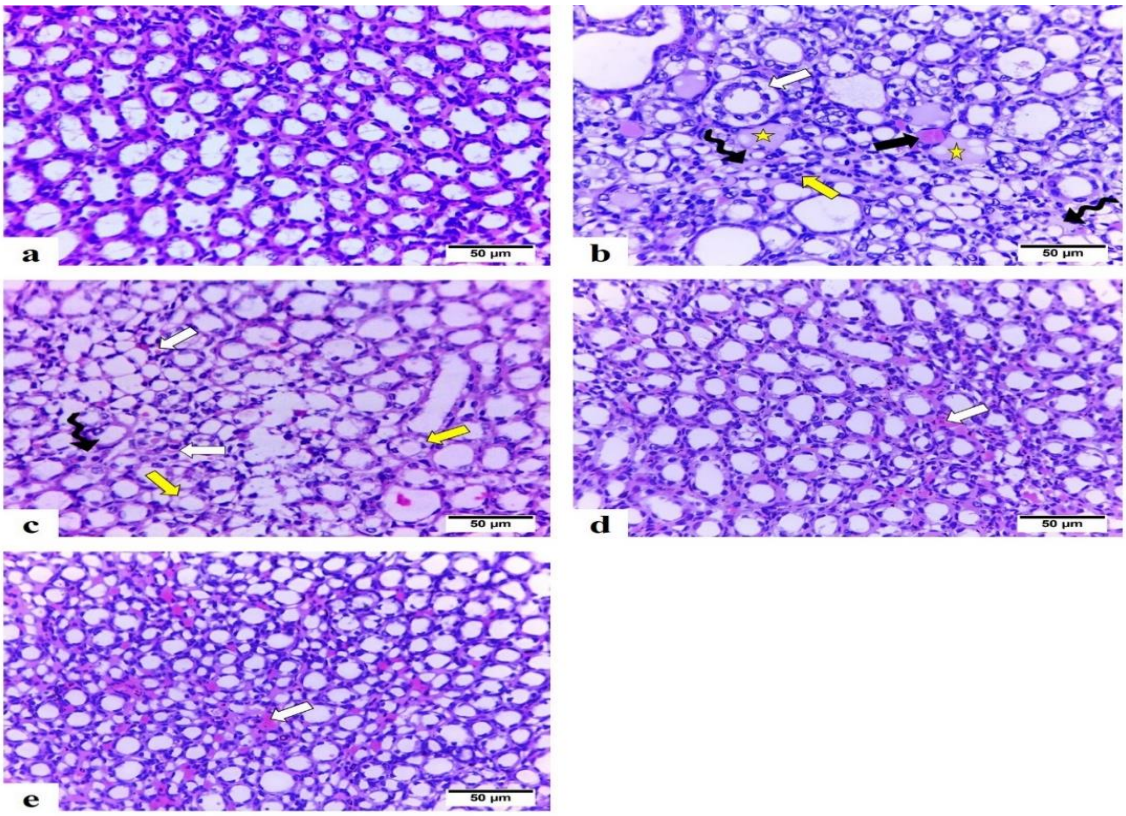

Fig. 6. Representative photomicrographs of sections of renal medulla from different experimental groups (H & E):

(a) Control group displays normal architecture of collecting tubules. (b) GM-treated group reveals severe vacuolar degeneration of collecting tubules (white arrow), interstitial inflammatory infiltrates (yellow arrow), congestion (black arrow), edema (wave arrow) and hyaline casts (star). (c) LDE+ GM-treated group shows mild vacuolar degeneration in collecting tubules (yellow arrow), edema (wave arrow) and congestion (white arrow). (d) HDE+ GM-treated group as well as (e) NAC+ GM-treated group exhibit apparently normal cytoarchitecture of collecting tubules. However, congestion (white arrow) is also observed but with less extent.

As illustrated in **(Table 5)**, the GM-treated group showed the substantially highest lesion score at *p value* less than 0.05 compared to the control group. On the other hand, the severity of lesions significantly ($p < 0.05$) reduced in the groups co-treated with the low dose of *M. fruticosum extract*, high dose of *M. fruticosum* extract, and NAC. Interestingly, there was no significant difference between the control and high dose of *M. fruticosum* extract.

Table 5. Histopathological lesion score in different experimental groups:

Parameters	C	GM	LDE+GM	HDE+GM	NAC+GM
Tubular degeneration	0 ± 1	4 ± 1[a]	2 ± 1[abc]	1 ± 1[b]	1.5 ± 1[abc]
Tubular necrosis	0 ± 1	3 ± 1[a]	1 ± 1[abc]	0 ± 1[b]	1 ± 1[b]
Inflammation	0 ± 0	3 ± 1[a]	1 ± 1[abc]	0 ± 1[b]	1 ± 0[abc]
Hyalinization	0 ± 0	2 ± 1[a]	0 ± 1[b]	0 ± 1[b]	0 ± 1[b]

Values are presented as median ± interquartile range (n=8 rats/group). [a] Significantly different from control, [b] Significantly different from GM-treated group, [c] Significantly different from HDE + GM-treated group, the same superscript letters in the same row are considered insignificant. The statistical analysis was conducted by using Kruskal-Wallis test and the Mann-Whitney U test.

3.11. Immunohistochemistry

3.11.1. Caspase 3

As depicted in **Fig 7a.**, the control group showed negative caspase-3 immune expression. However, the GM-treated group demonstrated strong positive caspase-3 immunoreactivity **(Fig. 7b)**. Conversely, LDE + GM group displayed moderate immune expression **(Fig. 7c)** whereas both HDE + GM and NAC + GM groups revealed mild caspase 3 immunoreactivity **(Fig. 7d and e, respectively)**.

The immune expression of caspase 3 was significantly ($P < 0.05$) higher in the GM-treated group with a mean area % of 27.39 ± 0.71 compared to the control group. In contrast, the co-treated groups (LDE, HDE, and NAC) exhibited a substantial ($P < 0.05$) reduction in caspase 3 immunoreactivity with mean area % values of 15.68 ± 0.42, 11.99 ± 0.38, and 11.09 ± 0.30, respectively. Notably, the LDE + GM group showed significantly ($P < 0.05$) higher immune expression compared to the HDE + GM and NAC + GM groups. However, the HDE + GM group did not exhibit significant immune reactivity compared to the NAC + GM group ($P > 0.05$) **(Fig. 7)**.

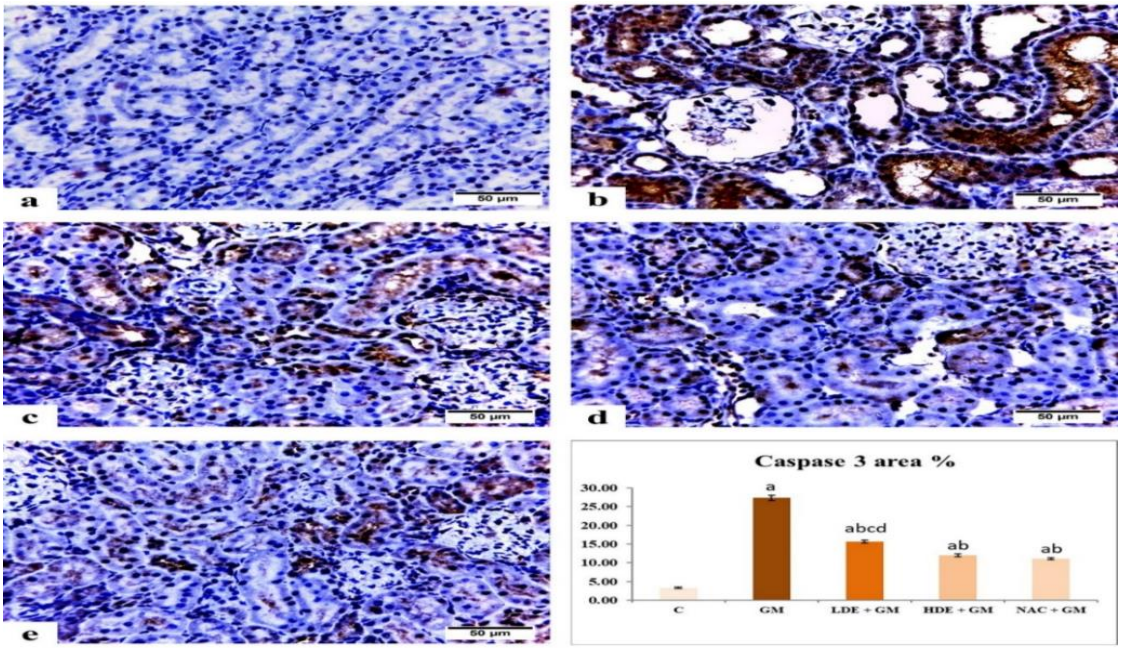

Fig. 7. Photomicrograph of renal tissue sections representing caspase 3 immune expression in different treated groups:

(a) Control group showing negative immune expression. (b) GM-treated group demonstrating strong positive caspase 3 immunoreactivity. (c) LDE+ GM-treated group displaying moderate immune expression. (d) HDE+ GM-treated group revealing mild caspase 3 immunoreactivity. (e) NAC + GM-treated group exhibiting mild caspase 3 immune expression. Chart presenting quantification of positive immune expression as area percent. Values are expressed as mean ± SEM (n=8rats/group). [a] Significantly different from control group, [b] Significantly different from GM-treated group, [c] Significantly different from HDE + GM-treated group, [d] Significantly different from NAC+ GM-treated group at $P \leq 0.05$.

3.11.2. NF-κB

As presented in **Fig 8a.**, the control group showed negative NF-κB immune expression. However, the GM-treated group demonstrated strong positive NF-κB immunoreactivity **(Fig. 8b)**. Conversely, LDE + GM group displayed moderate immune expression **(Fig. 8c)** whereas both HDE + GM and NAC + GM groups revealed mild NF-κB immunoreactivity **(Fig. 8d and e, respectively)**.

The immune expression of NF-$_k$B was significantly (P < 0.05) higher in the GM-treated group with a mean area % of 15.46 ± 0.52 compared to the control group. In contrast, the co-treated groups (LDE, HDE, and NAC) exhibited a substantial (P < 0.05) reduction in NF-$_k$B immunoreactivity with mean area % values of 9.37 ± 0.23, 7.51 ± 0.12, and 7.46 ± 0.19, respectively. Notably, the LDE + GM group showed significantly (P < 0.05) higher immune expression compared to the HDE + GM and NAC + GM groups. However, the HDE + GM group did not exhibit significant immune reactivity compared to the NAC + GM group (P > 0.05) **(Fig. 8)**.

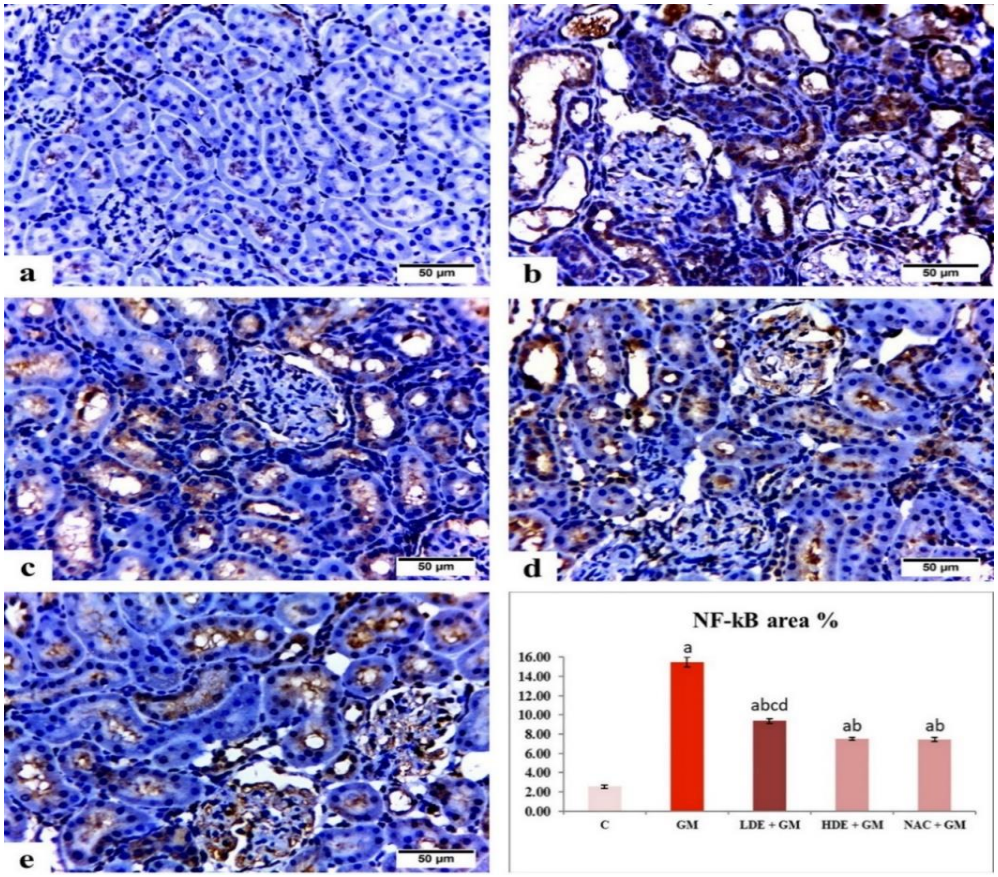

Fig. 8. Photomicrograph of renal tissue sections representing NF-kB immune expression in different treated groups:

(a) Control group showing negative immune expression. (b) GM-treated group demonstrating strong positive NF-kB immunoreactivity. (c) LDE+ GM-treated group displaying moderate immune expression. (d) HDE+ GM-treated group revealing mild NF-kB immunoreactivity. (e) NAC + GM -treated group exhibiting mild NF-kB immune expression. Chart presenting quantification of positive immune expression as area percent. Values are expressed as mean ± SEM (n=8rats/group). [a] Significantly different from control group, [b] Significantly different from GM-treated group, [c] Significantly different from HDE+ GM-treated group, [d] Significantly different from NAC+ GM-treated group at $P \leq 0.05$.

4. Discussion

The results of the present work demonstrated the protective effects of the *M. fruticosum* leaves methanolic extract against GM-induced nephrotoxicity. GM injection produced marked renal injury, as evidenced by elevated markers of kidney function, along with the marked decrease in the antioxidant enzyme activities and the concomitant increase in the renal lipid peroxidation, and NO levels, these data are consistent with previous studies [2, 42]. The marked increase in levels of serum urea, BUN, creatinine, and BUN/Creatinine ratio compared to normal control indicated impaired kidney function due to decreased glomerular filtration rate (GFR). Previous research has shown that GM reduces GFR by inducing tubular apoptosis, necrosis, and inflammation, leading to decreased blood flow to the kidneys. Additionally, GM affects renal hemodynamics by causing vasoconstriction of the afferent arteriole, resulting in reduced blood flow and pressure in the glomerulus, leading to a decreased GFR [8, 43]. High serum levels of creatinine and urea indicate glomerular impairment while high proteinuria implies renal tubular damage [44].

However, co-administration of *M. fruticosum* methanolic extract with GM significantly ameliorated the abnormalities in kidney function parameters, particularly with the use of a 400 mg/kg dose of the extract, which exhibited amelioration effects comparable to or greater than the reference drug. By investigating the chemical profile of the methanolic extract, it was found to be rich in flavonoids and phenolics. These phytochemical constituents have been shown in several studies to inhibit increased serum creatinine and BUN levels, as well as urinary excretion of total protein, due to their antioxidant properties [45-47].

Additionally, our findings indicated that GM administration significantly increased markers indicative of oxidative stress in the kidneys, including MPO and MDA, while decreasing the activity of antioxidant enzymes SOD, CAT, and GST, as well as GSH levels, these results are consistent with previous studies [1, 48]. GM-induced renal toxicity primarily occurs due to oxidative stress caused by the increased production of reactive nitrogen and oxygen species (ROS), redox imbalance, as well as reduced antioxidant capacity in the kidneys [8].

In the current study, GM significantly raised renal MPO activity which generates more ROS and reactive nitrogen species that can suppress the renal activities of SOD, CAT, GST, and GSH, increase renal MDA level; a biomarker of oxidative stress and a bioactive trigger of inflammation and ultimately contributing to renal damage by damaging cellular components such as proteins, DNA, and lipids.

Our study further demonstrated a noteworthy inverse correlation between renal MDA and the activities of renal antioxidant enzymes. The correlation coefficients between MDA and SOD, GST, CAT, and GSH were -0.894**, -0.771**, -0.814**, and -0.79**, respectively (**$P < 0.01$). These findings underscore the significance of antioxidant therapies in the management of renal diseases characterized by oxidative damage, such as those induced by GM exposure.

Interestingly, the co-treatment with methanolic extract, particularly at a dose of 400 mg/kg, significantly attenuated the GM-induced oxidative stress in the renal tissues. This was evidenced by improved renal activities of antioxidant enzymes, as well as levels of MDA, and MPO, and favourable histopathological results compared to the GM-treated group. *In vitro* tests revealed that the extract has potent scavenging activity against free radicals, suggesting its potential as an antioxidant (Fig. 1). The extract's abundant profile of phenolics and flavonoids is likely responsible for its antioxidant activity. Flavonoids and phenolics are widely known for their antioxidant properties and can work through various mechanisms such as reducing the production of ROS, scavenging free radicals, modulating antioxidant enzyme activity, chelating metal ions, and regulating signal transduction pathways and gene expression related to antioxidant defence [49, 50]. These findings support the possibility of using *M. fruticosum* leaves methanolic extract as a potential therapy against renal diseases induced by oxidative damage.

Moreover, administration of GM significantly increased renal levels of NO, NF-kB, TNF-α, IL-6, and caspase 3, indicating the inflammatory and cell apoptotic effects of GM. These findings were supported by histopathological changes and immunohistochemical results. Our results are in line with previous research [2], [51-53] demonstrating that GM-induced oxidative damage can further lead to inflammation and apoptosis through various cellular signaling pathways, including NF-kB, inducible nitric oxide synthase (iNOS), and caspase-3. Specifically, GM-induced oxidative stress can activate iNOS, leading to the overproduction of NO, which can react with superoxide radicals to form peroxy-nitrite, a highly reactive molecule known to cause tissue damage and inflammation and aggravate renal failure [54]. Furthermore, NO can activate the

NF-kB pathway, resulting in the production of pro-inflammatory cytokines TNF-α and IL-6 [55].

Our results demonstrated a noteworthy inverse correlation between renal NO and the activities of renal antioxidant enzymes. The correlation coefficients between NO and SOD, GST, CAT, and GSH were -0.775**, -0.617**, -0.639**, and -0.68** respectively (**$P < 0.01$).

According to previous studies, GM can activate caspase-3, a key enzyme involved in the renal apoptotic pathway, through the intrinsic mitochondrial pathway and activation of TNF-α, IL-6, and NF-k_B. TNF-α and IL-6 can activate NF-k_B, which can promote the expression of pro-apoptotic genes and activate caspase-3 [52, 56, 57].

Furthermore, our study found that GM-induced renal injury led to increased plasma levels of liver enzymes indicating potential liver damage. This observation aligns with previous research showing that GM-induced nephrotoxicity can have remote effects on other organs, including the liver [8, 58].

Additionally, the histopathological examination confirmed the oxidative and inflammatory effects of GM on renal tissues, showing severe renal damage such as glomerular degeneration and atrophy, widening of renal tubules with squamous epithelial cells lining, vacuolar degeneration of renal tubules, desquamation of epithelial lining, and hyalinization. These findings are consistent with previous studies [2, 59, 60]. Increased intracellular H_2O and Na ions from an imbalance in fluid equilibrium induce leakage of lysosomal enzymes causing cytoplasmic degradation, macromolecular crowding, and vacuolar degeneration of lining epithelia [61,62]. The desquamation of lining epithelia may be due to oxidative stress induced by GM, resulting in cell-cell separation [63]. GM predominantly induces cytoplasmic vacuolation, tubular necrosis, and exfoliation of epithelial lining due to prominent endocytic activity and abundant lysosomes and mitochondria of the epithelia lining PCT [64]. The presence of hyaline casts in the kidneys may indicate protein metabolism disruption caused by renal damage [65]. Furthermore, the GM-treated group showed severe interstitial inflammatory infiltrates, suggesting that the GM may interact with the enzymes and proteins of interstitial tissues, triggering the overproduction of ROS and inhibiting the antioxidant defense, subsequently increasing the migration of inflammatory cells, and stimulating inflammation [66, 67].

Interestingly, all the above changes were reversed using the *M. fruticosum* leaves methanolic extract which significantly reduced renal levels of inflammatory markers such as NO, NF-kB, TNF-α, and IL-6, as well as caspase 3. The extract also improved the histopathological changes and immunohistochemical analysis related to inflammation and apoptosis induced by GM administration. Both low and high doses of the extract were effective, with the high dose of 400 mg/kg showing results like those of the reference drug. Also, the results suggested that the administration of *M. fruticosum* extract could alleviate hepatic disturbances resulting from GM-induced nephrotoxicity. This beneficial effect might be attributed to the extract's antioxidative and anti-inflammatory properties, which may act on the kidney and/or directly on the liver.

The primary components of the extract were identified using the UPLC/ESI-QTOF-MS/MS technique and included melodamide A, kaempferol, quercetin, rutin, luteolin, apigenin, and chrysin. These components have been previously reported to exhibit antioxidant, anti-inflammatory, and anti-apoptotic effects, which may be responsible for the extract's protective effects on the kidneys. Melodamide A, a phenolic amide found in the extract, has demonstrated potent anti-inflammatory activity by inhibiting the pro-inflammatory function of human neutrophils [41]. Kaempferol, a well-known flavonol, has potent antioxidant, anti-apoptotic, anti-inflammatory, and nephroprotective activities, preventing nephropathy and restoring normal kidney lipid levels [68, 69]. Additionally, quercetin exhibited antioxidant, anti-inflammatory, and anti-apoptotic capabilities, and microglial activation-induced apoptosis [70, 71]. Rutin, quercetin 3-rutinoside, a famous powerful anti-inflammatory and anti-apoptotic can alter oxidative stress biomarkers, downregulate iNOS, and enhance the expression of Nrf2 [72, 73]. Luteolin, a common flavone in many vegetables, fruits, and medicinal plants, alleviates nephrotoxicity through antioxidant, anti-inflammatory, and Nrf2/ARE/HO-1 overexpression pathways [74], as well as downregulating NF-B and TNF and modulating tubular cells' apoptosis [45]. Chrysin, another identified flavone in *M. fruticosum*, possesses protective effects against renal damage induced by paracetamol, and doxorubicin [75, 76]. Chrysin lowers the levels of DNA damage markers and modulators COX-2, 8-OHdG, and KIM-1 compared to untreated subjects [77]. Chrysin also has been reported to have a nephroprotective role in the prevention of cyclosporine A -induced renal fibrosis [78]. Moreover, apigenin exhibits antioxidant, anti-inflammatory, and anti-apoptotic effects, mitigating cisplatin-induced nephrotoxicity [79]. Naringenin can trigger antioxidant reactions, inhibit the release of pro-inflammatory cytokines [80], and attenuate lead-induced kidney damage in rats [81]. Pinocembrin, the

flavanone precursor of chrysin, mitigates GM-induced nephrotoxicity in rats by improving kidney function and inhibiting oxidative stress as well as apoptotic conditions [82]. Pinocembrin treatment ameliorates diabetic nephropathy, as it improves lipid profile, glomerular filtration rate and urinary protein, it also avoids increases in urinary biomarkers, oxidative stress, and glomerular basement membrane thickness [83]. Ferulic acid, the predominant hydroxycinnamic acid in plants, has nephroprotective effects in GM-induced nephrotoxicity through diminishing inflammation and oxidative stress [84]. Overall, these components make the extract of *M. fruticosum* a potential therapeutic agent for renal diseases.

5. Conclusion

The present study demonstrated for the first time the nephroprotective effect of *M. fruticosum* leaves methanolic extract against GM-induced kidney damage in rats via modulating several signaling pathways in a dose-dependent manner. Certainly, *M. fruticosum* leaves methanolic extract inhibits NO and NF-κB levels and attenuates both inflammatory cytokines (IL-6 and TNF-α) and apoptotic marker (caspase 3) along with inhibiting the immunohistochemical expression of NF-κB and caspase 3 via alleviating oxidative stress, augmenting the activities of antioxidant enzymes (SOD, GST, CAT, and GSH) concomitantly with diminishing lipid peroxidation (MDA levels) induced by GM. Furthermore, co-administration of the methanolic extract with GM significantly ameliorated kidney function parameters (urea, BUN, creatinine, and BUN/Creatinine ratio) and alleviated all histological changes. This beneficial effect may be attributed to the phytochemical constituents identified by UPLC/ESI-QTOF-MS/MS technique. Therefore, *M. fruticosum* leaves methanolic extract may serve as a potential therapy against renal diseases induced by oxidative damage.

6. Abbreviations

ALT: Alanine Aminotransferase
AST: Aspartate Aminotransferase
BUN: Blood Urea Nitrogen
CAT: Catalase
GM: Gentamicin
GSH: Reduced Glutathione
GST: Glutathione-S-Transferase
IL-6: Interleukin 6
MDA: Malondialdehyde
MPO: Myeloperoxidase
NAC: N-acetyl Cysteine
NF-κB: Nuclear Factor Kappa B
NO: Nitric Oxide
ROS: Reactive Oxygen Species
SOD: Superoxide Dismutase
TNF-α: Tumor Necrosis Factor-Alpha
UPLC/ESI-QTOF-MS/MS: Ultraperformance Liquid Chromatography/Electrospray Ionization-Quadrupole Time-of-Flight Tandem Mass Spectrometry

7. Conflict of interests

The authors declare that they have no conflict of interests.

8. Funding resources

This research was conducted without any external financial support.

9. References

[1] Martin J, Barras M, Yui NA, Kirkpatrick C, Kubler P, Norris R (2012) Gentamicin monitoring practices in teaching hospitals–time to undertake the necessary randomised controlled trial. J Clin Toxicol 2(8):146-1. http://doi.org/10.4172/2161-0495.1000146

[2] Ince S, Kucukkurt I, Demirel HH, Arslan-Acaroz D, Varol N (2020) Boron, a trace mineral, alleviates gentamicin-induced nephrotoxicity in rats. Biol Trace Elem Res 195(2):515-24. https://doi.org/10.1007/s12011-019-01875-4

[3] Kang C, Lee H, Hah D-Y, Heo JH, Kim CH, Kim E, et al (2013) Protective effects of *Houttuynia cordata* Thunb. on gentamicin-induced oxidative stress and nephrotoxicity in rats. Toxicological research 29:61-7. https://doi.org/10.5487%2FTR.2013.29.1.061

[4] Mazzon E, Britti D, De Sarro A, Caputi AP, Cuzzocrea S (2001) Effect of N-acetylcysteine on gentamicin-mediated nephropathy in rats. Eur J Pharmacol 424(1):75-83. https://doi.org/10.1016/s0014-2999(01)01130-x

[5] Sassen M, Kim S, Kwon T-H, Knepper M, Miller R, Frøkiaer J, et al (2006) Dysregulation of renal sodium transporters in gentamicin-treated rats. Kidney Int 70(6):1026-37. https://doi.org/10.1038/sj.ki.5001654

[6] Veljković M, Pavlović DR, Stojiljković N, Ilić S, Jovanović I, Poklar Ulrih N, et al (2017) Bilberry: chemical profiling, *in vitro* and *in vivo* antioxidant activity and nephroprotective effect against gentamicin toxicity in rats. Phytother Res 31(1):115-23. https://doi.org/10.1002/ptr.5738

[7] Bae EH, Kim IJ, Joo SY, Kim EY, Choi JS, Kim CS, et al (2014) Renoprotective effects of the direct renin inhibitor aliskiren on gentamicin-induced nephrotoxicity in rats. JRAAS 15(4):348-61. https://doi.org/10.1177/1470320312474853

[8] Mohamadi Yarijani Z, Najafi H, Shackebaei D, Madani SH, Modarresi M, Jassemi SV (2019) Amelioration of renal and hepatic function, oxidative stress, inflammation and histopathologic damages by *Malva sylvestris* extract in gentamicin induced renal toxicity. Biomed Pharmacother 112:108635. https://doi.org/10.1016/j.biopha.2019.108635

[9] Chinnappan SM, George A, Thaggikuppe P, Choudhary Y, Choudhary VK, Ramani Y, et al (2019) Nephroprotective effect of herbal extract *Eurycoma longifolia* on paracetamol-induced nephrotoxicity in rats. Evid Based Complement Alternat Med 2019. https://doi.org/10.1155/2019/4916519

[10] Pripdeevech P, Chukeatirote E (2010) Chemical compositions, antifungal and antioxidant activities of essential oil and various extracts of *Melodorum fruticosum* L. flowers. Food Chem Toxicol 48(10):2754-8. https://doi.org/10.1016/j.fct.2010.07.002

[11] Engels NS, Waltenberger B, Schwaiger S, Huynh L, Tran H, Stuppner H (2019) Melodamide A from *Melodorum fruticosum*—quantification using HPLC and one-step-isolation by centrifugal partition chromatography. J Sep Sci 42(20):3165-72. https://doi.org/10.1002/jssc.201900392

[12] Do LT, Sichaem J (2022) New Flavonoid Derivatives from *Melodorum fruticosum* and Their α-Glucosidase Inhibitory and Cytotoxic Activities. Molecules 27(13):4023. https://doi.org/10.3390/molecules27134023

[13] Soni A, Sosa S (2013) Phytochemical analysis and free radical scavenging potential of herbal and medicinal plant extracts. J Pharmacogn Phytochem 2(4):22-9.

[14] Brand-Williams W, Cuvelier M-E, Berset C (1995) Use of a free radical method to evaluate antioxidant activity. LWT-Food science and Technology 28(1):25-30. https://doi.org/10.1016/S0023-6438(95)80008-5

[15] Finney DJ (1971) A statistical treatment of the sigmoid response curve. Probit analysis Cambridge University Press, London 633.

[16] Zilić S, Serpen A, Akıllıoğlu G, Gökmen V, Vančetović J (2012) Phenolic compounds, carotenoids, anthocyanins, and antioxidant capacity of colored maize (*Zea mays* L.) kernels. J Agric Food Chem 60(5):1224-31. https://doi.org/10.1021/jf204367z

[17] Junejo JA, Rudrapal M, Nainwal LM, Zaman K (2017) Antidiabetic activity of hydro-alcoholic stem bark extract of *Callicarpa arborea* Roxb. with antioxidant potential in diabetic rats. Biomed Pharmacother 95:84-94. https://doi.org/10.1016/j.biopha.2017.08.032

[18] Abo-Elghiet F, Ibrahim MH, El Hassab MA, Bader A, Abdallah QMA, Temraz A (2022) LC/MS analysis of *Viscum cruciatum* Sieber ex Boiss. extract with anti-proliferative activity against MCF-7 cell line via G0/G1 cell cycle arrest: An in-silico and in-vitro study. J Ethnopharmacol 295:115439. https://doi.org/10.1016/j.jep.2022.115439

[19] El-Tantawy WH, Soliman ND, El-Naggar D, Shafei A (2015) Investigation of antidiabetic action of *Antidesma bunius* extract in type 1 diabetes. Arch Physiol Biochem 121(3):116-22. https://doi.org/10.3109/13813455.2015.1038278

[20] Falayi OO, Oyagbemi AA, Omobowale TO, Ayodele EA, Adedapo AD, Yakubu MA, et al (2018) Nephroprotective properties of the methanol stem extract of *Abrus precatorius* on gentamicin-induced renal damage in rats. J Complementary Integr Med 16(3):20170176. https://doi.org/10.1515/jcim-2017-0176

[21] Feng D, Huang H, Yang Y, Yan T, Jin Y, Cheng X, et al (2015) Ameliorative effects of N-acetylcysteine on fluoride-induced oxidative stress and DNA damage in male rats' testis. MRGTEM 792:35-45. https://doi.org/10.1016/j.mrgentox.2015.09.004

[22] Waterborg JH (2009) The Lowry method for protein quantitation. The protein protocols handbook, pp 7-10.

[23] Ellman GL (1959) Tissue sulfhydryl groups. Arch Biochem Biophys 82(1):70-7. https://doi.org/10.1016/0003-9861(59)90090-6

[24] Uchiyama M, Mihara M (1978) Determination of malonaldehyde precursor in tissues by thiobarbituric acid test. Anal Biochem 86(1):271-8. https://doi.org/10.1016/0003-2697(78)90342-1

[25] Marklund S, Marklund G (1974) Involvement of the superoxide anion radical in the autoxidation of pyrogallol and a convenient assay for superoxide dismutase. Eur J Biochem 47(3):469-74. https://doi.org/10.1111/j.14321033.1974.tb03714.x

[26] Claiborne A (1985) Handbook of methods for oxygen radical research. Florida: CRC Press, Boca Raton, pp 283-4.

[27] Habig WH, Pabst MJ, Jakoby WB (1974) Glutathione S-transferases: the first enzymatic step in mercapturic acid formation. J Biol Chem 249(22):7130-9. https://doi.org/10.1016/S0021-9258(19)42083-8

[28] Green LC, Wagner DA, Glogowski J, Skipper PL, Wishnok JS, Tannenbaum SR (1982) Analysis of nitrate, nitrite, and [15N] nitrate in biological fluids. Anal Biochem 126(1):131-8.

[29] Goldblum SE, Wu K-M, Jay M (1985) Lung myeloperoxidase as a measure of pulmonary leukostasis in rabbits. J Appl Physiol 59(6):1978-85. https://doi.org/10.1016/0003-2697(82)90118-x

[30] Bellavite P, Dri P, Bisiacchi B, Patriarca P (1977) Catalase deficiency in myeloperoxidase deficient polymorphonuclear leucocytes from chicken. FEBS Lett 81(1):73-6. https://doi.org/10.1016/0014-5793(77)80931-9

[31] Bancroft JD, Gamble M (2008) Theory and practice of histological techniques: Elsevier health sciences.

[32] Khalaf AAA, Elhady MA, Hassanen EI, Azouz AA, Ibrahim MA, Galal MK, et al (2021) Antioxidant role of carvacrol against hepatotoxicity and nephrotoxicity induced by

propiconazole in rats. Revista Brasileira de Farmacognosia 31:67-74. http://dx.doi.org/10.1007/s43450-021-00127-8

[33] Noshy PA, Yasin NAE, Rashad MM, Shehata AM, Salem FMS, El-Saied EM, et al (2023) Zinc nanoparticles ameliorate oxidative stress and apoptosis induced by silver nanoparticles in the brain of male rats. Neurotoxicology 95:193-204. https://doi.org/10.1016/j.neuro.2023.02.005

[34] Abdel-Daim MM, Farouk SM, Madkour FF, Azab SS (2015) Anti-inflammatory and immunomodulatory effects of *Spirulina platensis* in comparison to *Dunaliella salina* in acetic acid-induced rat experimental colitis. Immunopharmacol Immunotoxicol 37(2):126-39. https://doi.org/10.3109/08923973.2014.998368

[35] Ye M, Yan Y, Guo D-a (2005) Characterization of phenolic compounds in the Chinese herbal drug Tu-Si-Zi by liquid chromatography coupled to electrospray ionization mass spectrometry. Rapid Commun Mass Spectrom 19(11):1469-84. https://doi.org/10.1002/rcm.1944

[36] Ding S, Dudley E, Plummer S, Tang J, Newton R, Brenton A (2008) Fingerprint profile of *Ginkgo biloba* nutritional supplements by LC/ESI-MS/MS. Phytochemistry 69(7):1555-64. https://doi.org/10.1016/j.phytochem.2008.01.026

[37] Fabre N, Rustan I, de Hoffmann E, Quetin-Leclercq J (2001) Determination of flavone, flavonol, and flavanone aglycones by negative ion liquid chromatography electrospray ion trap mass spectrometry. J Am Soc Mass Spectrom 12(6):707-15. https://doi.org/10.1016/s1044-0305(01)00226-4

[38] Jung J, Pummangura S, Chaichantipyuth C, Patarapanich C, McLaughlin J (1990) Bioactive constituents of *Melodorum fruticosum*. Phytochemistry 29(5):1667-70. https://doi.org/10.1016/0031-9422(90)80142-4

[39] Mbakidi-Ngouaby H, Pinault E, Gloaguen V, Costa G, Sol V, Millot M, et al (2018) Profiling and seasonal variation of chemical constituents from *Pseudotsuga menziesii* wood. Ind Crops Prod 117:34-49. http://dx.doi.org/10.1016/j.indcrop.2018.02.069

[40] Hong Y, Wang Z, Barrow CJ, Dunshea FR, Suleria HA (2021) High-throughput screening and characterization of phenolic compounds in stone fruits waste by lc-esi-qtof-ms/ms and their potential antioxidant activities. Antioxidants 10(2):234. https://doi.org/10.3390/antiox10020234

[41] Chan H-H, Hwang T-L, Thang TD, Leu Y-L, Kuo P-C, Nguyet BTM, et al (2013) Isolation and synthesis of melodamide A, a new anti-inflammatory phenolic amide from the leaves of *Melodorum fruticosum*. Planta Med 79(03/04):288-94. https://doi.org/10.1055/s-0032-1328131

[42] El-Tantawy WH, Mohamed SA-H, Abd Al Haleem EN (2013) Evaluation of biochemical effects of *Casuarina equisetifolia* extract on gentamicin-induced nephrotoxicity and oxidative stress in rats. Phytochemical analysis. J Clin Biochem Nutr 53(3):158-65. https://doi.org/10.3164/jcbn.13-19

[43] Randjelovic P, Veljkovic S, Stojiljkovic N, Sokolovic D, Ilic I (2017) Gentamicin nephrotoxicity in animals: current knowledge and future perspectives. EXCLI journal 16:388. https://doi.org/10.17179/excli2017-165

[44] Ranasinghe R, Mathai M, Zulli A (2023) Cytoprotective remedies for ameliorating nephrotoxicity induced by renal oxidative stress. Life Sci 318:121466. https://doi.org/10.1016/j.lfs.2023.121466

[45] Domitrović R, Cvijanović O, Pugel EP, Zagorac GB, Mahmutefendić H, Škoda M (2013) Luteolin ameliorates cisplatin-induced nephrotoxicity in mice through inhibition of platinum accumulation, inflammation and apoptosis in the kidney. Toxicology 310:115-23. https://doi.org/10.1016/j.tox.2013.05.015

[46] Mir SM, Ravuri HG, Pradhan RK, Narra S, Kumar JM, Kuncha M, et al (2018) Ferulic acid protects lipopolysaccharide-induced acute kidney injury by suppressing inflammatory events and upregulating antioxidant defenses in Balb/c mice. Biomed Pharmacother 100:304-15. https://doi.org/10.1016/j.biopha.2018.01.169

[47] Hu T, Yue J, Tang Q, Cheng K-W, Chen F, Peng M, et al (2022) The effect of quercetin on diabetic nephropathy (DN): A systematical review and Meta-analysis of animal studies. Food Funct 13:4789. https://doi.org/10.1039/d1fo03958j

[48] Harisa GI, Abo-Salem OM (2012) Benfotiamine ameliorate gentamicin-induced nephrotoxicity: effect on renal oxidative stress markers and plasma platelets activating factor acylhydrolase activity. Int J Pharmacol 8(5):364-72. https://doi.org/10.3923/ijp.2012.364.372

[49] Van Hung P (2016) Phenolic compounds of cereals and their antioxidant capacity. Crit Rev Food Sci Nutr 56(1):25-35. https://doi.org/10.1080/10408398.2012.708909

[50] de Oliveira NK, Almeida MRS, Pontes FMM, Barcelos MP, de Paula da Silva CHT, Rosa JMC, et al (2019) Antioxidant effect of flavonoids present in Euterpe *oleracea Martius* and neurodegenerative diseases: A literature review. Cent Nerv Syst Agents Med Chem 19(2):75-99. https://doi.org/10.2174/1871524919666190502105855

[51] Kalkan Y, Kapakin KAT, Kara A, Atabay T, Karadeniz A, Simsek N, et al (2012) Protective effect of *Panax ginseng* against serum biochemical changes and apoptosis in kidney of rats treated with gentamicin sulphate. J Mol Histol 43(5):603-13. https://doi.org/10.1007/s10735-012-9412-4

[52] El Gamal AA, AlSaid MS, Raish M, Al-Sohaibani M, Al-Massarani SM, Ahmad A, et al (2014) Beetroot (*Beta vulgaris* L.) extract ameliorates gentamicin-induced nephrotoxicity associated oxidative stress, inflammation, and

apoptosis in rodent model. Mediators Inflamm 2014:983952. https://doi.org/10.1155/2014/983952

[53] Subramanian P, Anandan R, Jayapalan JJ, Hashim OH (2015) Hesperidin protects gentamicin-induced nephrotoxicity via Nrf2/HO-1 signaling and inhibits inflammation mediated by NF-κB in rats. J Funct Foods 13:89-99. https://doi.org/10.1016/j.jff.2014.12.035

[54] Christo JS, Rodrigues AM, Mouro MG, Cenedeze MA, de Jesus Simões M, Schor N, et al (2011) Nitric oxide (NO) is associated with gentamicin (GENTA) nephrotoxicity and the renal function recovery after suspension of GENTA treatment in rats. Nitric Oxide 24(2):77-83. https://doi.org/10.1016/j.niox.2010.12.001

[55] Baig MS, Zaichick SV, Mao M, de Abreu AL, Bakhshi FR, Hart PC, et al (2015) NOS1-derived nitric oxide promotes NF-κB transcriptional activity through inhibition of suppressor of cytokine signaling-1. J Exp Med 212(10):1725-38. https://doi.org/10.1084/jem.20140654

[56] Chen Y-C, Chen C-H, Hsu Y-H, Chen T-H, Sue Y-M, Cheng C-Y, et al (2011) Leptin reduces gentamicin-induced apoptosis in rat renal tubular cells via the PI3K-Akt signaling pathway. Eur J Pharmacol 658(2-3):213-8. https://doi.org/10.1016/j.ejphar.2011.02.025

[57] Abo-Elghiet F, Mohamed SA, Yasin NAE, Temraz A, El-Tantawy WH, Ahmed SF (2023) The effect of *Alnus incana* (L.) Moench extracts in ameliorating iron overload-induced hepatotoxicity in male albino rats. Sci Rep 13(1):7635. https://doi.org/10.1038/s41598-023-34480-6

[58] Al-Asmari AK, Abbasmanthiri R, Al-Elewi AM, Al-Omani S, Al-Asmary S, Al-Asmari SA (2014) Camel milk beneficial effects on treating gentamicin induced alterations in rats. J Toxicol 2014:917608. https://doi.org/10.1155/2014/917608

[59] Salem EA, Salem NA, Kamel M, Maarouf AM, Bissada NK, Hellstrom WJ, et al (2010) Amelioration of gentamicin nephrotoxicity by green tea extract in uninephrectomized rats as a model of progressive renal failure. Ren Fail 32(10):1210-5. https://doi.org/10.3109/0886022x.2010.517350

[60] Quirós Y, Blanco-Gozalo V, Sanchez-Gallego JI, López-Hernandez FJ, Ruiz J, de Obanos MPP, et al (2016) Cardiotrophin-1 therapy prevents gentamicin-induced nephrotoxicity in rats. Pharmacol Res 107:137-46. https://doi.org/10.1016/j.phrs.2016.02.025

[61] Del Monte U(2005) Swelling of hepatocytes injured by oxidative stress suggests pathological changes related to macromolecular crowding. Med Hypotheses 64(4):818-25. https://doi.org/10.1016/j.mehy.2004.08.028

[62] Aboelwafa HR, Ramadan RA, Ibraheim SS, Yousef HN (2022) Modulation Effects of Eugenol on Nephrotoxicity Triggered by Silver Nanoparticles in Adult Rats. Biology 11(12):1719. https://doi.org/10.3390/biology11121719

[63] Inumaru J, Nagano O, Takahashi E, Ishimoto T, Nakamura S, Suzuki Y, et al (2009) Molecular mechanisms regulating dissociation of cell–cell junction of epithelial cells by oxidative stress. Genes Cells 14(6):703-16. https://doi.org/10.1111/j.1365-2443.2009.01303.x

[64] Stojiljkovic N, Stoiljkovic M, Randjelovic P, Veljkovic S, Mihailovic D. (2012) Cytoprotective effect of vitamin C against gentamicin-induced acute kidney injury in rats. Exp Toxicol Pathol 64(1-2):69-74. https://doi.org/10.1016/j.etp.2010.06.008

[65] Abdelhalim MAK, Moussa SAA (2013) The gold nanoparticle size and exposure duration effect on the liver and kidney function of rats: *In vivo*. Saudi J Biol Sci 20(2):177-81. https://doi.org/10.1016%2Fj.sjbs.2013.01.007

[66] Gałażyn-Sidorczuk M, Brzóska MM, Jurczuk M, Moniuszko-Jakoniuk J (2009) Oxidative damage to proteins and DNA in rats exposed to cadmium and/or ethanol. Chem Biol Interact 180(1):31-8. https://doi.org/10.1016/j.cbi.2009.01.014

[67] Iqbal M, Okazaki Y, Okada S (2009) Curcumin attenuates oxidative damage in animals treated with a renal carcinogen, ferric nitrilotriacetate (Fe-NTA): implications for cancer prevention. Mol Cell Biochem 324(1):157-64. https://doi.org/10.1007/s11010-008-9994-z

[68] Langeswaran K, Selvaraj J, Ponnulakshmi R, Mathaiyan M, Vijayaprakash S (2018) Protective effect of Kaempferol on biochemical and histopathological changes in mercuric chloride induced nephrotoxicity in experimental rats. J Biol Act Prod Nat 8(2):125-36. http://dx.doi.org/10.1080/22311866.2018.1451386

[69] Alagal RI, AlFaris NA, Alshammari GM, ALTamimi JZ, AlMousa LA, Yahya MA (2022) Kaempferol attenuates doxorubicin-mediated nephropathy in rats by activating SIRT1 signaling. J Funct Foods 89:104918. https://doi.org/10.1016/j.jff.2021.104918

[70] Ishikawa Y, Kitamura M (2000) Anti-apoptotic effect of quercetin: intervention in the JNK-and ERK-mediated apoptotic pathways. Kidney Int 58(3):1078-87. https://doi.org/10.1046/j.15231755.2000.00265.x

[71] Sanchez-Gonzalez PD, Lopez-Hernandez FJ, Duenas M, Prieto M, Sanchez-Lopez E, Thomale J, et al (2017) Differential effect of quercetin on cisplatin-induced toxicity in kidney and tumor tissues. Food Chem Toxicol 107:226-36. https://doi.org/10.1016/j.fct.2017.06.047

[72] Radwan RR, Fattah SMA (2017) Mechanisms involved in the possible nephroprotective effect of rutin and low dose γ irradiation against cisplatin-induced nephropathy in rats. J Photochem Photobiol, B 169:56-62. https://doi.org/10.1016/j.jphotobiol.2017.02.022

[73] Singh HP, Singh TG, Singh R (2021) Evaluation of the renoprotective effect of syringic acid against nephrotoxicity induced by cisplatin in

rats. J Appl Pharm Sci 11(1):80. http://dx.doi.org/10.7324/JAPS.2021.11s109

[74] Alekhya Sita GJ, Gowthami M, Srikanth G, Krishna MM, Rama Sireesha K, Sajjarao M, et al (2019) Protective role of luteolin against bisphenol A-induced renal toxicity through suppressing oxidative stress, inflammation, and upregulating Nrf2/ARE/HO-1 pathway. IUBMB Life 71(7):1041-7. https://doi.org/10.1002/iub.2066

[75] Rashid S, Ali N, Nafees S, Ahmad ST, Arjumand W, Hasan SK, et al (2013) Alleviation of doxorubicin-induced nephrotoxicity and hepatotoxicity by chrysin in Wistar rats. Toxicol Mech Methods 23(5):337-45. https://doi.org/10.3109/15376516.2012.759306

[76] Kandemir FM, Kucukler S, Eldutar E, Caglayan C, Gülçin İ (2017) Chrysin protects rat kidney from paracetamol-induced oxidative stress, inflammation, apoptosis, and autophagy: a multi-biomarker approach. Sci Pharm 85(1):4. https://doi.org/10.3390/scipharm85010004

[77] Ijaz MU, Jabeen F, Ashraf A, Imran M, Ehsan N, Samad A, et al (2022) Evaluation of possible protective role of Chrysin against arsenic-induced nephrotoxicity in rats. Toxin Reviews 41(4):1237-45. http://dx.doi.org/10.1080/15569543.2021.1993261

[78] Nagavally RR, Sunilkumar S, Akhtar M, Trombetta LD, Ford SM (2021) Chrysin ameliorates cyclosporine-A-induced renal fibrosis by inhibiting TGF-β1-induced epithelial–mesenchymal transition. Int. J. Mol. Sci. 22(19):10252. https://doi.org/10.3390/ijms221910252

[79] Ju SM, Kang JG, Bae JS, Pae HO, Lyu YS, Jeon BH (2015) The flavonoid apigenin ameliorates cisplatin-induced nephrotoxicity through reduction of p53 activation and promotion of PI3K/Akt pathway in human renal proximal tubular epithelial cells. Evid Based Complement Alternat Med 2015:186436. https://doi.org/10.1155/2015/186436

[80] Manchope MF, Ferraz CR, Borghi SM, Rasquel-Oliveira FS, Franciosi A, Bagatim-Souza J, et al (2022) Therapeutic role of naringenin to alleviate inflammatory pain. Treatments, mechanisms, and adverse reactions of anesthetics and analgesics: Elsevier, pp 443-55. https://doi.org/10.1016/B978-0-12-820237 1.00038-7

[81] Wang J, Li T, Feng J, Li L, Wang R, Cheng H, et al (2018) Kaempferol protects against gamma radiation-induced mortality and damage via inhibiting oxidative stress and modulating apoptotic molecules *in vivo* and *vitro*. Environ Toxicol Pharmacol 60:128-37. https://doi.org/10.1016/j.etap.2018.04.014

[82] Promsan S, Jaikumkao K, Pongchaidecha A, Chattipakorn N, Chatsudthipong V, Arjinajarn P, et al (2016) Pinocembrin attenuates gentamicin-induced nephrotoxicity in rats. Can J Physiol Pharmacol 94(08):808-18. https://doi.org/10.1139/cjpp-2015-0468

[83] Granados-Pineda J, Uribe-Uribe N, García-López P, Ramos-Godinez MDP, Rivero-Cruz JF, Pérez-Rojas JM (2018) Effect of pinocembrin isolated from mexican brown propolis on diabetic nephropathy. Molecules 23(4):852. https://doi.org/10.3390/molecules23040852

[84] Erseckin V, Mert H, İrak K, Yildirim S, Mert N (2022) Nephroprotective effect of ferulic acid on gentamicin-induced nephrotoxicity in female rats. Drug Chem Toxicol 45(2):663-9. https://doi.org/10.1080/01480545.2020.1759620